IOP Conf. Series: Materials Science and Engineering **194** (2017) 012004 doi:10.1088/1757-899X/194/1/012004

Strength, corrosion resistance, and biocompatibility of ultrafine-grained Mg alloys after different modes of severe plastic deformation

S V Dobatkin[1,2*], E A Lukyanova[1,2], N S Martynenko[1], N Yu Anisimova[3], M V Kiselevskiy[3], M V Gorshenkov[1], N Yu Yurchenko[4], G I Raab[5], V S Yusupov[2], N Birbilis[6], G A Salishchev[4], Y Z Estrin[1,6]

[1] Laboratory of Hybrid Nanostructured Materials, National University of Science and Technology "MISIS", Moscow, 119991, Russia
[2] A.A. Baikov Institute of Metallurgy and Materials Science of the Russian Academy of Sciences, Moscow, 119334, Russia
[3] N.N. Blokhin Russian Cancer Research Center, Moscow, 115478, Russia
[4] Belgorod National Research University, Belgorod, 308015, Russia
[5] Ufa State Aviation Technical University, Ufa, 45008, Russia
[6] Department of Materials Science and Engineering, Monash University, Melbourne, VIC 3800, Australia

*E-mail: dobatkin.sergey@gmail.com

Abstract. The effect of severe plastic deformation on the structure, mechanical properties, corrosion resistance, and biocompatibility of the WE43 (Mg-Y-Nd-Zr) alloy earmarked for applications as bioresorbable material has been studied. The alloy was deformed by rotary swaging (RS), equal channel angular pressing (ECAP), and multiaxial deformation (MAD). The microstructure examination by transmission electron microscopy showed that all SPD modes lead to the formation of ultrafine-grained structure with a structural element size of 0.5-1 μm and the $Mg_{12}Nd$ phase particles 0.3 μm in size. The microstructure refinement by all three treatments resulted in strengthening of the alloy. ECAP and MAD also raised ductility to up to 12-17%, while RS increased the ultimate tensile strength to up to 415 MPa. The study of the corrosion properties showed that SPD does not affect the electrochemical corrosion of the alloy. Its biocompatibility *in vitro* was estimated after incubation of the samples with red blood cells (hemolysis study), white blood cells (cell viability assay), and mesenchymal stromal cells (cell proliferation analysis). The biodegradation rate in fetal bovine serum was also evaluated. ECAP and MAD were found to cause some deceleration of biodegradation by slowing down the gas formation in the biological fluid and, compared to MSC, to improve the biocompatibility of the WE43 alloy.

1. Introduction

Over the past decade, magnesium and its alloys have attracted a great deal of attention as possible medical implant materials [1, 2]. Their potential for medical applications, particularly in bioresorbable implants, owes to their low density, high specific strength, and good biocompatibility. However, because of its high chemical activity, magnesium is characterized by a high corrosion rate, which is accompanied by the active evolution of hydrogen gas [3]. Such disadvantages limit the use of magnesium alloys as materials for bioresorbable implants. The WE43 alloy containing rare earth

metals (REMs) is one of the most popular medical magnesium alloys [4]. Alloying with REMs improves the corrosion resistance of magnesium [5] and also enhances its strength. Another method of increasing the strength characteristics is severe plastic deformation (SPD), which leads to the formation of ultrafine-grained (UFG) structure in magnesium and its alloys [6]. Such structure provides substantial strengthening [6-9] and also leads to improved corrosion resistance and reduced gas evolution. The reduction of gas evolution, in turn, gives rise to improved biocompatibility, which expands the suitability of WE43 alloy as a biodegradable implant material.
In this work, the WE43 alloy was processed by rotary swaging (RS), equal-channel angular pressing (ECAP), and multiaxial deformation (MAD). The effect of deformation on the microstructure, mechanical properties and corrosion resistance of the alloy has been studied, and its biocompatibility *in vitro* has been evaluated in the initial state and after the deformation by the three SPD modes.

2. Experimental

The material studied in this work was a Mg-3.56% Y-2.20% Nd-0.47% Zr (wt %) alloy. In the initial state, the alloy was homogenized at a temperature of 525°C for 8 hours. This was followed by deformation by various SPD methods, including rotary swaging, multiaxial deformation, and equal-channel angular pressing. The processing schemes are shown in Fig. 1. Deformation was performed at gradually decreasing temperature and increasing degree of strain. In the case of RS, temperature was decreased from 425°C to 350°C in 25°C steps, and the cumulative equivalent strain reached a level of 1.02. MAD was performed on workpieces 25 mm in diameter and 40 mm in length in an Instron 300LX universal hydraulic testing machine at a low rate of 1 mm/min. Again, deformation was performed in several steps, with successive drops in temperature of 25°C from 450°C to 300°C. The total number of deformation cycles was 28. ECAP was performed using a die with an angle of 120° between the channels with stepwise drops in temperature from 425°C to 300°C at the final 12th pass. The cumulative equivalent strain in the ECAP billets (10 mm in diameter and 80 mm in length) was about 7.6.

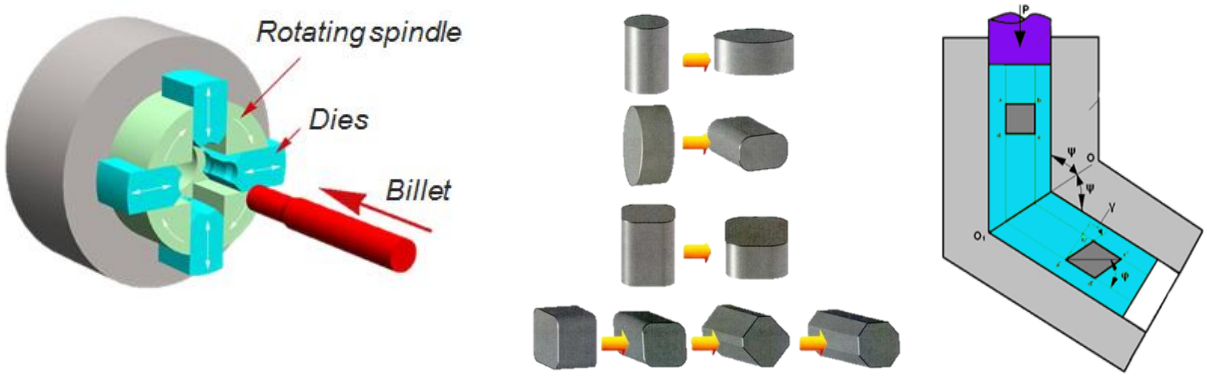

a b c

Figure 1. Schemes of deformation processing of the alloy: (a) RS, (b) MAD, and (c) ECAP.

The structure of the alloy after homogenization was examined with a Reichert MeF optical microscope. The TEM analysis of the alloy after SPD was carried out with a JEM 1400 transmission electron microscope operating at a voltage of 120 kV. The room temperature mechanical properties before and after deformation were measured in tension on cylindrical samples with a 3 mm diameter and 15 mm gage length in an Instron 1096 machine at an extension rate of 1.5 mm/min.
The potentiodynamic polarization (PDP) method was used to evaluate the corrosion resistance of the alloy. The PDP tests were performed with a VMP potentiostat under the control of EC-Lab specialized software (Bio-logic). The unit used a standard flat cell with three electrodes (working electrode, saturated calomel reference electrode, and Pt-mesh counter electrode). The corrosive medium was 0.9% NaCl solution in water. Before testing, all surfaces were ground to 2000 grit by sandpaper.

To study biocompatibility and biodegradation, samples 2 mm thick and 8 mm in diameter were sanded on sandpaper (P2000) and then polished on a wet cloth. Prior to testing, the samples were sterilized by steam in an autoclave at 120°C for 30 minutes and then washed three times with RPMI-1640 (PanEco, Russia) sterile medium.

For hemolysis studies, anticoagulated CBA mouse whole blood was centrifuged at 1000 rpm for 10 min at 20°C for removal of plasma. Then red blood cells (RBCs) were washed for additional three times with phosphate buffered saline (PBS), pH 7.4, for 5 min. Washed RBCs were mixed with PBS (1:9) and used within 2 h for the hemolysis assay as described by A.V. Maximkin et al. [10]. 1000 μL of RBCs suspension were introduced into a well of a 24-well plate with the sample. Positive and negative controls were produced by adding 100 μL of Triton-X-100 (Sigma-Aldrich, USA) or PBS, respectively. The plate with RBCs and alloy samples was incubated at 37°C. Probes for analysis were collected 1, 2, 3, 4, 5, 6, 24 h after start of the test and centrifuged at 300 rpm for 3 min. Optical density (OD) of the supernatant was measured at 540 nm using a Labsystems Multiscan MS plate reader. The percentage hemolysis was calculated from the calibration curve.

For evaluation of the effect of alloys on cell vitality, 1 ml of mouse white blood cells (WBCs) in RPMI-1640 medium supplemented with 10% fetal bovine serum (Thermo Scientific, USA), 100 μg/ml penicillin, 100 μg/mL streptomycin, and 2 mM L-glutamine (all-Gibco, USA) at a density of 5×10^5 cells/cm^2 were cultivated with alloy samples in a 24-well plate (Nunc, USA) at 37°C in a humidified atmosphere with 5% CO_2. The control WBCs were treated only with RPMI 1640. After incubation for 2 and 24 h, 20 μL 3- (4.5-dimethylthiazol-2-yl)-2.5-diphenyltetrazolium bromide (MTT) (Sigma) with a concentration of 5 mg·mL^{-1}, was added into each well. The plates were incubated for 4 h under cell culture conditions. Subsequently, 500 μL dimethyl sulphoxide (PanEco, Russia) was added to the cells by replacing the medium, to dissolve the formazan crystals. OD of the solution (100 μL) was measured at 540 nm in 96-well plates. The vitality of WBCs was calculated using the following formula:

$$Vitality, \% = OD\ samples/OD\ control \times 100.$$

Mesenchymal stromal/stem cells (MSCs) were isolated according to the standard techniques for the isolation of mononuclear cells from bone marrow of CBA mouse femurs using density gradient centrifugation [11]. The cells were cultured in Dulbecco's modified Eagle's medium (DMEM, high glucose) (Gibco), supplemented with 10% fetal bovine serum (FBS) in a humidified incubator at 95% relative humidity and 5% CO_2 at 37°C. Cells were passaged at about 80%-90% confluency. For the experiments, cells after the third passage were used. Cells were tested with flow cytometry for the presence of characteristic markers on BD FACSCanto II Cells Analyzer (Becton Dickinson). We used the specific CD105, CD90, CD45 and CD34 antibodies (Becton Dickinson or Bioscience). MSCs were trypsinized by TryplE (Life Technologies, USA) and seeded in wells at a density of 1×10^5 cells. The 24-wells plate containing tested alloy samples was incubated at 37°C in a humidified atmosphere for 5 days. At the end of the assay, MTT and dimethyl sulphoxide were added to each well as described earlier. The solution of each sample was placed in a microtiter plate, and the absorbance was measured in triplicate at 540 nm. OD baseline was measured during the first day of co-incubation of MSCs with alloy samples. The percentage of MSCs proliferation was calculated using the following formula:

$$Proliferation, \% = (Mean\ OD\ sample - Mean\ OD\ baseline)/Mean\ OD\ baseline \times 100.$$

In vitro degradation of the WE43 alloy after various SPD treatments (ECAP, MAD, RS) was evaluated after holding samples at 37°C in fetal bovine serum (FBS). To estimate the biodegradation rate, each WE43 alloy of (W_0) mg mass was immersed into 2 mL of FBS (HyClone UK Ltd., Thermo Scientific). The samples were placed into a CO_2 incubator (AutoFlow NU-4750 Water Jacket CO_2 Incubator, NuAire) at 37°C and 5% CO_2 for 1, 2, 3 and 4 weeks. Every week a sample of each type

was removed and washed ten times with distilled water. Then it was dried at a temperature of 20°C to a constant weight (W_{FBS}). The weight loss was defined as $W_{FBS}/W_0 \times 100\%$.
In order to assess the effect of the degree of surface preparation on the corrosion properties and biocompatibility of the alloy, we measured roughness parameters such as the arithmetic average roughness (R_a), the root mean square roughness (R_q), the average maximum peak-to-valley value (R_z), and the average maximum height of the profile (R_t). The kurtosis (R_{ku}) and skewness (R_{sk}) characteristics describing the shape and distribution of peaks [12] were also determined. The roughness measurements were carried out using a WYKO NT 1100 optical profilometer (Veeco Instruments, USA). The measurements were performed by vertical scanning interferometry. The average roughness was measured on a surface area of 900 μm x 1200 μm for each state of the alloy.

3. Results and Discussion

Upon homogenization, a uniform grain structure with an average grain size of 70 μm is formed in the WE43 alloy. In addition, the structure contains a small amount of the $Mg_{12}Nd$ phase, which was not dissolved upon homogenization (Fig. 2a). All three types of SPD result in similar microstructures of the alloy with close average grain sizes of 0.73 ± 0.21 μm after ECAP, 0.61 ± 0.19 μm after RS, and 0.93 ± 0.29 μm after MAD (Figs. 2b, 2c, and 2d). The size of the $Mg_{12}Nd$ particles precipitated upon heating for processing and upon deformation is 0.3 μm for all three types of SPD. It should also be noted that the microstructure of the samples that underwent RS exhibited an increased dislocation density and deformation twins. In this case, $Mg_{24}Y_5$ phase platelets are observed in addition to the globular $Mg_{12}Nd$ phase particles.

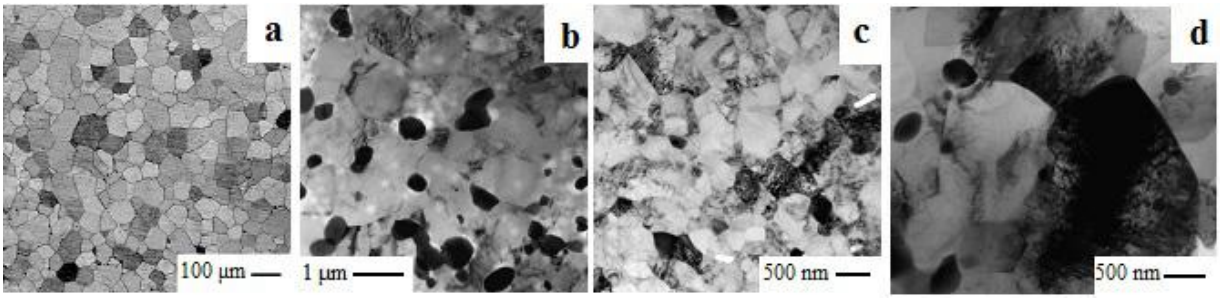

Figure 2. Structure of the WE43 alloy (a) in the initial state and (b)-(d) after different SPD treatments: (b) ECAP, (c) RS, and (d) MAD

The mechanical properties were measured at room temperature by uniaxial tensile tests. Table 1 presents the values yield strength, ultimate tensile strength, and tensile elongation returned by the tests. It can be seen that SPD processing causes a substantial increase in the strength of the alloy. In addition, ECAP and MAD also increase tensile ductility to 12.4% and 17.2%, respectively. It should also be noted that the combination of refined grains, deformation twins, and increased dislocation density in the structure after RS led to a nearly two-fold strength of the alloy.

Table 1. Mechanical properties of WE43 alloy in the initial state and after different SPD treatments

Treatment	UTS, MPa	YS, MPa	El, %
Homogenization at 525°C, 8 h	220	150	10.2
Rotary swaging (RS)	415	285	7.0
Multiaxial deformation (MAD)	300	210	17.2
Equal channel angular pressing (ECAP)	300	260	12.4

The resistance to electrochemical corrosion was estimated at room temperature by potentiodynamic tests. Figure 3 shows the polarization curves after various treatments of the alloy in comparison with the initial state. It can be seen that the corrosion resistance is not compromised by the severe deformation of the alloy. Table 2 summarizes the data on the corrosion potential E_{corr} and the corrosion current density i_{corr}, as determined from the Tafel plots, for the alloy in the initial state and after various SPD treatments. The data obtained show that the best corrosion resistance of the alloy is achieved by MAD. In this case, a slight increase in the corrosion potential is observed, which indicates an increase in the corrosion resistance. At the same time, the corrosion current density remains at the level of the initial, undeformed state.

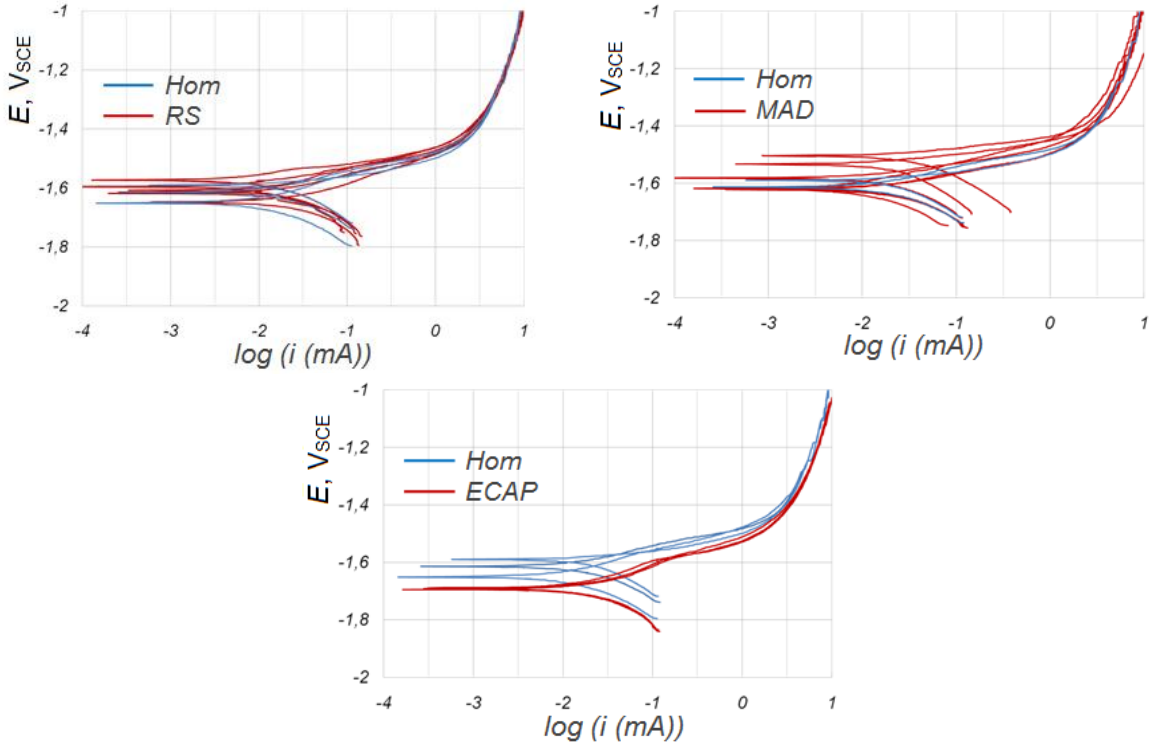

Figure 3. Polarization curves (potential *E* in volts with respect to a saturated calomel electrode (SCE) *vs.* current *i*) for the WE43 alloy in the initial homogenized state ("Hom") and after various SPD treatments.

Table 2. Results of PDP tests of the WE43 alloy in the initial state and after different SPD treatments

Treatment	E_{corr}, mV_{SCE}	i_{corr}, $\mu A/cm^2$
Homogenization at 525°C, 8 h	-1630 ± 34	21.3 ± 4.5
Rotary swaging (RS)	-1686 ± 8	29.8 ± 6.5
Multiaxial deformation (MAD)	-1595 ± 38	21.9 ± 8.9
Equal channel angular pressing (ECAP)	-1608 ± 27	30.0 ± 11.6

The hemolysis characteristics were tested for 1, 2, 3, 4, 5, and 24 hours after the incubation of the WE43 alloy samples with RBC (red blood cells) (Fig. 4a). It should be noted that all SPD treatments of the WE43 alloy decelerate the hemolysis to some extent as compared to the initial undeformed

state. The lowest value of the hemolysis after the incubation time of 1 hour is reached for the alloy after ECAP and MAD: 4-5% and 8-9% compared to 80% in the undeformed state. However, with increasing incubation time, the sample processed by ECAP shows a rapid increase of the hemolysis. In the case of MAD, the hemolysis level increased more slowly than in the case of other treatments. After 5 hours of incubation, the hemolysis level of the samples after MAD was substantially lower than in other test samples.

Figure 4b presents the viability of WBCs evaluated before and after the SPD treatments. A sharp decrease in the viability of WBCs is observed already after 2 hours of incubation for a homogenized sample and an RS treated one. By contrast, samples of ECAP and MAD processed material had virtually no effect on the cell viability. After 24 hours, a significant decrease in the viability of WBCs was recorded for all SPD treatments. Note that the lowest (30%) and the highest (60%) viability levels were exhibited by the homogenized alloy and the alloy processed by MAD, respectively.

According to Fig. 4c, all WE43 samples cause a strong inhibition of MSCs proliferation. The greatest cytotoxicity to bone marrow MSCs was exhibited by the samples of homogenized alloy and those after RS treatment, whilst no significant difference was observed between these two conditions: -22% and -18% MSC proliferation, respectively. The samples after ECAP and MAD did exhibit a lower MSC proliferation: they showed 17% and 2%, respectively.

Analysis of biodegradation of the alloy in embryonic bovine serum after various treatments showed the greatest mass loss for a sample that underwent RS. By contrast, the alloy samples after ECAP and MAD exhibited a very low degradation rate. In particular, after 4 weeks of incubation in the blood serum, the mass loss was 51.1 ± 0.07% after RS; 0.2 ± 0.04% after ECAP; and 0.02 ± 0.006% after MAD – to be compared with 5.5 ± 0.16% in the initial undeformed state (Fig. 4d). It should also be noted that the WE43 alloy in the undeformed condition and after RS processing exhibited long-term gas evolution upon incubation.

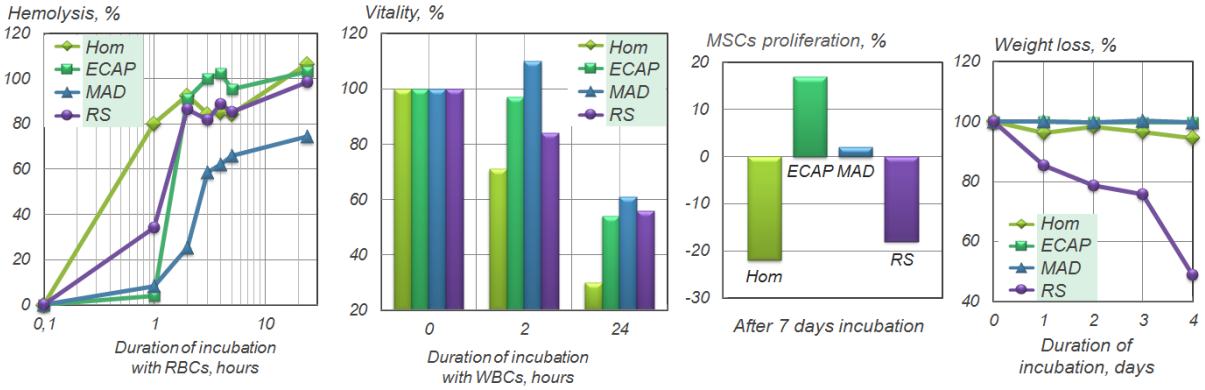

a b c d

Figure 4. Results of biocompatibility tests of the WE43 alloy in the initial state and after different SPD treatments.

The results of the surface roughness evaluation for the WE43 alloy after various treatments are presented in Fig. 5.

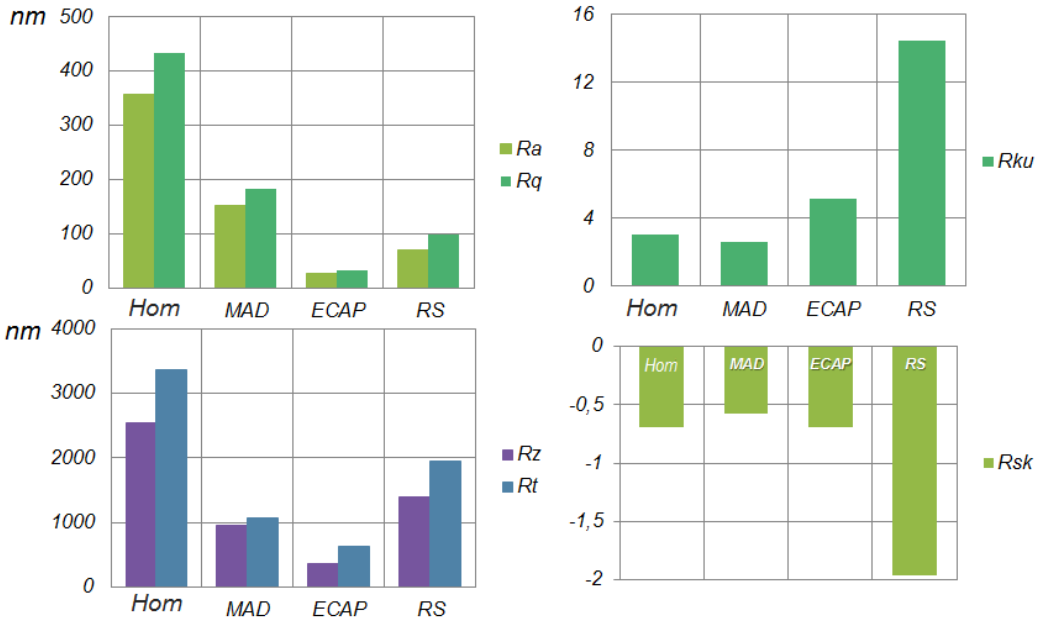

Figure 5. Surface roughness parameters of the WE43 alloy in the initial state and after different SPD treatments.

The surface roughness characteristics obtained in the work correlate with the results of the biocompatibility study. The R_a, R_t, R_z, and R_q parameters decreased after SPD in a way similar to a decrease in the hemolysis and an increase in the WBC viability and MSC proliferation relative to those of the undeformed state.

A closer look at kurtosis and skewness shows that these parameters are the largest for the samples after RS. This encourages the assumption that these parameters are the ones responsible for the extremely high biodegradation rate in the fetal serum even by comparison with that of the undeformed condition. Based on this correlation it can be surmised that the effect of SPD processing on biocompatibility of alloy WE43 can be associated with the differences in their surface morphology. These surface features are believed to be associated with the differences in the microstructures caused by SPD, particularly with regard to the grain size, dislocation density and the occurrence of deformation twins. Further studies substantiating this conjecture are certainly necessary.

4. Conclusions

1. Severe plastic deformation of the WE43 alloy by all three schemes leads to the formation of similar ultrafine-grained (UFG) structures characterized by a grain size of 0.5-1.0 μm and the presence of $Mg_{12}Nd$ phase particles 0.3 μm in size. Only the structure formed upon rotary swaging (RS) exhibited an increased dislocation density and deformation twins.

2. The UFG structure provides a high level of mechanical properties of the WE43 alloy. ECAP and MAD increase strength to 300 MPa to be compared with 220 MPa in the initial state. They also raise tensile ductility to a level of 12-17%. RS increases the ultimate tensile strength to 415 MPa, but at the cost of ductility.

3. The evaluation of the corrosion properties showed that SPD does not deteriorate the resistance to electrochemical corrosion.

4. Grain refinement by SPD predominantly improves the biocompatibility of the WE43 alloy.

As a general conclusion, it can be stated that SPD processing trialed in this study imparts to alloy WE43 a range of beneficial properties that qualify it as a candidate material for bioresorbable medical implants.

Acknowledgments
Part of this work relating to studies of biocompatibility was funded by the Ministry of Education and Science of the Russian Federation (grant #14.A12.31.0001) and the Increased Competitiveness Program of NUST «MISiS» (grant #K2-2016-062). Funding support of investigations of microstructure, mechanical performance, and corrosion properties was provided by the Russian Science Foundation (project #17-13-01488).

References

[1] Witte F, Zheng Y F and Gu X N 2014 *Mater. Sci.Eng. R* **77** p 1
[2] Hort N, Huang Y, Fechner D, Störmer M et al. 2010 *Acta Biomater.***6** 1714
[3] Kirkland N T, Birbilis N and Staiger M P 2012 *Acta Biomater.* **8** 925
[4] Liu Y, Zheng S, Li N, Guo H et al. 2016 *Mater. Lett.* **V179** 100
[5] Li N, Guo C, Wu Y H, Zheng Y F et al. 2012 *Corros. Eng. Sci. Techn.* **V47(5)** 346
[6] Lukyanova E A, Martynenko N S, Shakhova I E, Belyakov A N et al. 2016 *Mater. Lett.* **170** 5
[7] Salandari-Rabori A, Zarei-Hanzaki A, Fatemi S M, Ghambari M et al. 2011 J. *Alloys Compd.* **693** 409
[8] Diez M, Kim H-E, Serebryany V, Dobatkin S et al. 2014 *Mater. Sci.Eng. A* **V612** 287
[9] Zhang F, Zhang K-x, Tan C-w, YU X-d et al. 2011 *Trans. Nonferrous Met. Soc. China* **21** 2140
[10] Maksimkin AV, Senatov FS, Anisimova NYu et al. 2017 *Mater.Sci.Eng.* C **73** 366
[11] Yaochite J N, De Lima K W, Caliari-Oliveira C, Palma P V et al. 2016 *Stem Cell Res Ther.* **7(1)** 14.
[12] Gadelmawla E S, Koura M M, Maksoud T M A, Elewa I M et al. 2002 *J. Mater. Process. Technol.* **123** 133